

SIMPLIFIED DESIGN FLOW OF QUASI-OPTICAL SLOT AMPLIFIERS

I. Russo, L. Boccia, G. Amendola, and G. Di Massa

Dipartimento di Elettronica, Informatica e Sistemistica
Università della Calabria
Rende (CS) 87036, Italy

Abstract—Quasi-optical (QO) techniques have been extensively studied in recent years because of the promise they hold for medium and high power generation at millimeter- and sub-millimeter-wave frequencies, demonstrating higher efficiency than conventional approaches. In this work a step-by-step flow process is proposed for the design of a slot-based QO amplifier. The proposed design procedure is based on full-wave analysis of the individual building blocks, which are then cascaded to represent the whole system. An experimental assessment is proposed based on the design and on experimental analysis of the behavior of a C-band QO unit cell.

1. INTRODUCTION

In recent years, Quasi-optical (QO) systems have demonstrated [1] convincingly their ability to function as medium- and high-power sources at microwave and millimeter-wave frequencies. The true advantage of QO techniques lies in their unmatched ability to efficiently combine power from a large number of solid-state devices. Indeed, in QO systems the power from different sources is combined in free space, so signals are not affected by typical losses of printed circuits, losses which dramatically limit the efficiency of circuit-based power combiners.

Many research projects have been carried out in the field of QO power combining with a focus on amplifiers [2–5] and oscillators [6–8]. QO amplifiers, in particular, can be of two different types. A first type is represented by QO-grid amplifiers, which were first reported by Kim et al. [2], who demonstrated a 5×5 prototype operating at 3.3 GHz and based on packaged MESFETs. In this configuration, differentially fed

Corresponding author: I. Russo (irusso@deis.unical.it).

active devices are embedded into a regular grid composed of horizontal and vertical leads. A horizontally polarized incident wave excites RF current on the horizontal leads of the grid, driving the transistor pairs in a differential mode of operation. The amplified version of the input current flows on the vertical leads, causing the radiation of the orthogonally polarized beam toward the output of the system. Since this pioneering work, several others on grid amplifiers have been conducted and improvements in terms of efficiency, gain and operating frequency have been obtained employing monolithic circuits [5].

A second type of configuration, based on spatial power combining arrays, has been reported by various authors [9–14]. It consists of a periodic arrangement of unit cells, each one containing a transmitting and a receiving antenna connected to an amplifier stage. This architecture allows the use of more efficient radiators, which can be designed and optimized more effectively than in the grid case. However, the use of resonant elements increases the unit cell size, thus resulting in array-like behavior.

In this work, we present a simplified procedure for designing a spatial power-combining array. The structure taken as a reference is based on a pair of orthogonal slot antennas coupled to an amplifier through coplanar waveguides (CPWs) [9]. The active surface is placed within a resonant cavity formed by two orthogonal metal grating polarizers, which increase the achievable gain. Fabry-Perot cavities were used in [15, 16] to achieve high levels of the antenna gain. Key to the proposed simplified method is a division of the structure into several sub-blocks which can then be designed individually. As a result, the syntheses of the slot antennas, of the cavity, and of the common source amplifier stage can be approached separately and eventually combined to simulate the entire system. The proposed design flow has been experimentally validated by manufacturing and testing a unit cell of the spatial amplifier.

2. SLOT-BASED QUASI OPTICAL ARRAY

The QO amplifier configuration taken as a reference for this work is made up (Fig. 1) of an array of square unit cells, containing a pair of orthogonal slot antennas connected to each other by means of a common source amplifier [9].

The two antennas and the matching circuits are printed on a substrate of relative permittivity ϵ_1 and thickness h_1 . Amplification occurs when a vertically polarized wave excites the input slot antenna. The received signal is then driven to the intermediate amplifier stage through a Coplanar Waveguide (CPW) network printed on the same

board. The amplified current feeds the transmitting antenna, which is responsible for the radiation of the horizontally polarized output electric field \mathbf{E}_{out} .

Following the approach proposed by Popovic and York [9, 11], cross-polarization isolation between the input and output is achieved using metal-strip polarisers (shown in Fig. 2) that prevent spurious feedback oscillations and confine the beam to the forward direction. Both input and output polarizers are constructed on a dielectric

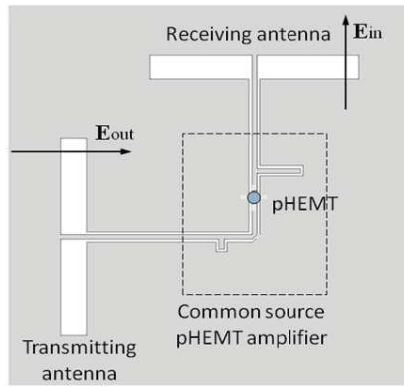


Figure 1. QO slot amplifier unit cell.

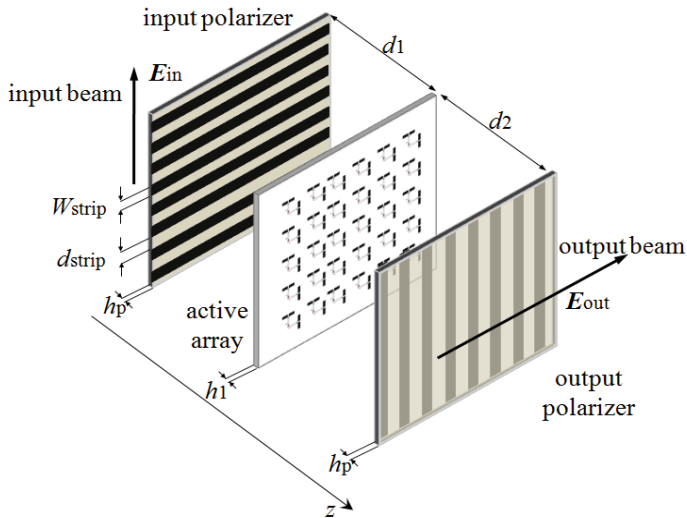


Figure 2. Transmission QO amplifier array.

substrate of relative permittivity ε_p and thickness h_p , with metal strips of width W_{strip} placed a distance d_{strip} apart. Thus, each polarizer acts as a polarization filter. In particular, the vertically polarized input signal, \mathbf{E}_{in} , passes through the input polarizer, exciting the input slot antenna. A portion of the power couples to the input slot antenna, is amplified and then, now vertically polarized, is reradiated toward the output polarizer. Another portion of the input wave is scattered by the input slot antenna and reflected by the output polarizer, which acts as a mirror for vertically polarized waves. The reflected signal travels back in the negative z direction, covering twice the distance d_1 . If d_1 is an odd multiple of $\lambda_0/4$, then the direct wave and the reflected wave sum constructively, resulting in increased power absorbed by each receiving slot. Similar behavior occurs for the horizontally polarized signal radiated by the output slot. Hence the polarizers reproduce a resonant cavity in the longitudinal direction, thus increasing both the output gain and the cross-polarization isolation between input and output fields.

3. DESIGN PROCEDURE

A QO amplifier can be designed using the unit-cell approach, with an infinite array scenario used to account for inter-element mutual coupling. The slot-based QO unit cell can thus be divided into different gain blocks as shown in Fig. 3. The first and the last stage take into account the losses L_{Pin} and L_{Pout} , of the input and output polarizer, respectively. The transmitting and receiving slot antennas are modeled by their respective gain, G_R and G_T , calculated within the resonant cavity. The central element is the common source amplifier, whose gain is G_A . Mismatching losses between the two antennas and the active device are taken into account by adding the blocks L_{RA} and L_{AT} . The overall gain of the cascade is indicated as G_{TOT} , and it corresponds to the entire gain of the QO amplifier for the transmission mode because the backward path is negligible since the signal is strongly confined in the forward direction by the polarizers and by the unilateral behavior of the active device. The behavior of the QO amplifier can therefore be

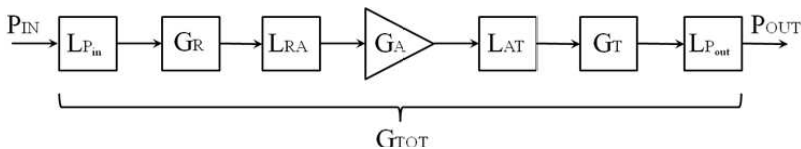


Figure 3. Amplification chain for the unit cell of the QO slot amplifier.

predicted by approaching one-by-one the individual stages, which can hence be designed separately. In the following discussion, the different design steps for the unit cell of a slot-based QO amplifier operating at 5 GHz are described.

3.1. Strip Grating Polarizers

Metal grating polarizers [17] are simple periodic polarization filters/frequency selective surfaces composed of metal strips of width W_{strip} and separated by a distance d_{strip} . Being periodic structures, they can be modeled using a unit-cell approach provided that E-wall and H-wall boundaries are chosen properly, as shown in Fig. 4. When the impinging electric field is cross-polarized with respect to the longitudinal direction of the metal strips, as shown in Fig. 4(a), the polarizer acts as a transparent surface. If the impinging electric field polarization has the same direction as the longitudinal dimension of the metal strips, as shown in Fig. 4(b), then the structure reflects

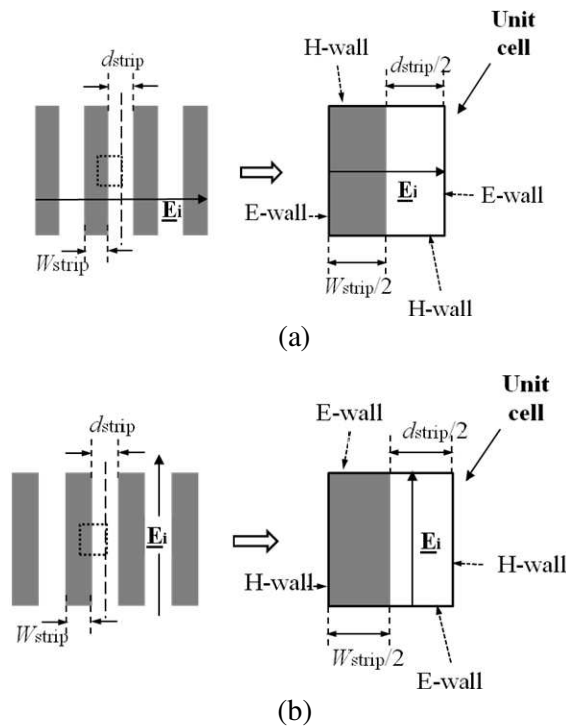


Figure 4. Polarizer unit cell models: (a) Transparent surface; (b) Reflecting surface.

almost all the incident power.

For the case at hand, polarizers were modeled using full-wave simulations. In particular, the strip width and inter-strip distance were optimized for the best tradeoff between high a transmission coefficient for the transparent operation mode, and a high reflection coefficient for the reflecting mode. A supporting Arlon CuClad 217 dielectric substrate with relative permittivity $\varepsilon_p = 2.17$ and thickness $h_p = 0.762$ mm was used. The optimized strip width was $W_{strip} = 1.8$ mm, and the inter-strip spacing was set at $d_{strip} = 0.6$ mm. Simulated transmission coefficients for both cases are reported in Fig. 5. The transparent operation mode showed a transmission coefficient, $L_{Pin} = L_{Pout}$, that was close to 0 dB across the whole frequency range considered during the analysis. As for the reflection operation mode, the transmission coefficient remained constantly below -45 dB.

3.2. Slot Antenna

The antenna type employed as receiving and transmitting element for the unit cell is a CPW-fed slot antenna [18–21]. There are several reasons for the choice of coplanar technology and a slot-style antenna. Indeed, using CPW technology, the integration of MMICs onto a coplanar structure is much easier and more practical than conventional microstrip lines, since there is no need for the via-hole connections that are required in active devices to apply ground potential to the reference terminals. The construction of CPWs turns out to be

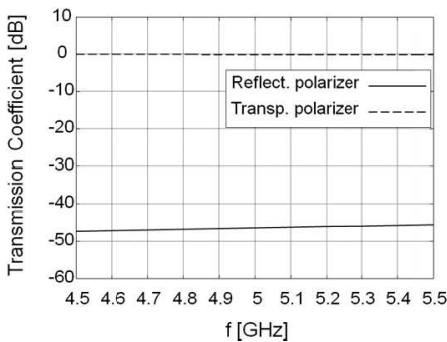


Figure 5. Simulated transmission coefficient for the transparent and reflecting polarizers.

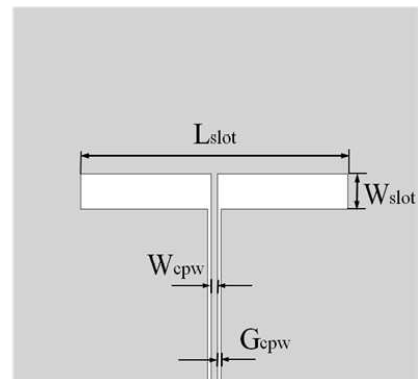


Figure 6. CPW-fed slot antenna layout.

relatively cheap because the circuit layout is simplified by the absence of multilayer connection holes. Furthermore, the absence of via-hole connections avoids the introduction of parasitic reactances. Finally, coplanar waveguides have lower radiation losses and less dispersion than microstrip lines.

The use of slot antennas, besides ensuring a significant bandwidth [19], follows naturally on the choice of coplanar technology.

The CPW-fed slot antenna layout is shown in Fig. 6. The antenna has been designed to operate within the C-band around the center frequency $f_0 = 5$ GHz. The structure has been constructed on a 1.6 mm-thick Arlon DiClad 870 substrate with relative permittivity $\epsilon_1 = 2.33$ and loss tangent $\tan \delta = 0.0012$ at a frequency of 5 GHz. The CPW feeding line was designed to have a characteristic impedance of 90Ω , obtained using an inner conductor of width $W_{strip} = 1$ mm and two gaps of width $G_{cpw} = 0.5$ mm. Simulations were performed using a full-wave commercial code [22] and including the polarizers located at a distance of $3/4\lambda_0$, thus limiting its perturbational effects on the antenna.

The antenna dimensions were optimized at the operating frequency of 5 GHz by setting the slot's length, L_{slot} , and width, W_{slot} , at 38.2 mm and 4.9 mm, respectively, for both the transmitter and the receiver element. Actual measurements were compared with simulated results, and the reflection coefficients are shown in Fig. 7. As can be observed, experimental and predicted results are in good agreement, both showing a -10 dB bandwidth that is slightly larger than 1 GHz

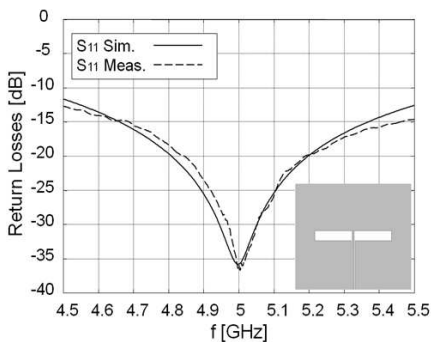


Figure 7. Simulated and measured slot antenna reflection coefficients.

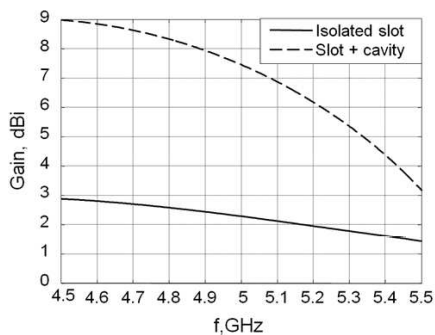


Figure 8. Simulated broadside gain comparison between the slot antenna in isolation and embedded into the resonant cavity.

around the operating frequency. The simulated antenna gain in the broadside direction, both with and without polarizers, is reported in Fig. 8. At 5 GHz, the isolated antenna has a gain of 2.5 dBi, but when the antenna is placed into the resonant cavity formed by the two orthogonal polarizers the gain improves to 7.6 dBi.

3.3. Common Source pHEMT Amplifier

The gain stage of the unit cell is a common source amplifier based on a low-noise pHEMT device [23]. The device used is a packaged pHEMT (model number FHX35LG) manufactured by Eudyina-Fujitsu. Because the device is surface-mounted, it can easily be soldered onto the CPW structure. The amplifier layout is depicted in Fig. 9. The dimensions used for the CPW are the same as those used for feeding the antennas. The solid-state device was matched to the $90\ \Omega$ characteristic impedance of the coplanar waveguide. The input and output matching networks were constructed using a series of open-shunt stubs. The dimensions of the stubs and lines were optimized through the use of a commercial hybrid-circuit/full-wave cosimulation environment [22,24] to find a good tradeoff among matching, bandwidth, and gain. The input and output stubs had a length of $L_{s1} = 8.2\ \text{mm}$ and $L_{s1} = 1.7\ \text{mm}$, respectively, while the input and output line lengths were $L_1 = 6.5\ \text{mm}$ and $L_{s1} + L_{s22} = 1.7\ \text{mm} + 1.8\ \text{mm}$, respectively. The amplifier was biased by applying a drain-to-source DC voltage of $V_{DS} = 2\ \text{V}$ and a DC drain current of $I_D = 10\ \text{mA}$.

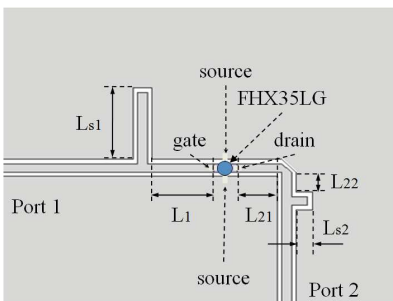


Figure 9. Common-source pHEMT amplifier layout.

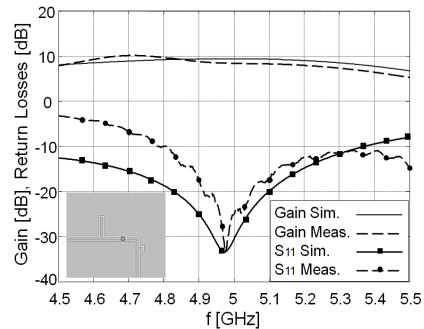


Figure 10. Gain and return losses of the simulated [19,21] and experimental analyses for the pHEMT common-source amplifier.

A prototype of the amplifier was fabricated and tested, and the measured and simulated results are reported in Fig. 10. As can be seen, there is good agreement between numerical and experimental data, with a good matching across a 500 MHz bandwidth around the center frequency and a measured gain of 8.4 dB at 5 GHz.

4. EXPERIMENTAL RESULTS

A prototype of the QO slot-based amplifier unit cell was fabricated and tested. In order to keep cross-coupling between the input and output slot antennas below 30 dB, the unit cell size, L_{cell} , was set at 65 mm, which corresponds to $1.08\lambda_0$ at 5 GHz. In principle, this unit-cell size is not well suited for array arrangements as it generates grating lobes. Hence it was chosen only for testing purposes. Indeed, it should be considered that unit-cell size can be further reduced by optimizing the layout, and grating lobes can be compensated for by using a non-rectangular lattice arrangement, which can also help by increasing inter-element spacing without introducing negative effects on the array radiation pattern.

A picture of the manufactured unit cell is shown in Fig. 11(a). A number of DC-decoupling chip capacitors (AVX model AccuP0603) with a nominal capacitance of 3.8 pF have been soldered between the gate terminal and the receiving slot and between the drain terminal and the transmitting slot. Furthermore, the bias potentials were applied by means of two turned wires, which act as inductors and impede the formation of RF-leakage currents in the direction of the DC bias generators. The final QO amplifier cavity is shown undergoing testing in Fig. 11(b).

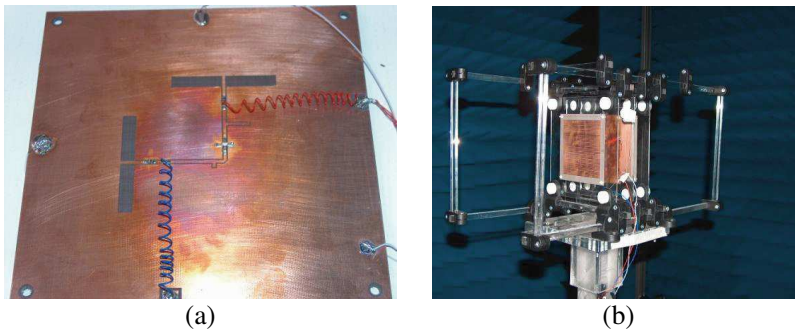


Figure 11. (a) The slot amplifier unit cell; (b) The complete system formed by the cavity and the active cell.

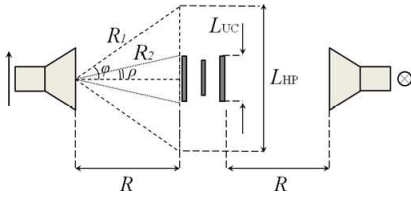


Figure 12. Measurement setup for evaluating the QO amplifier gain.

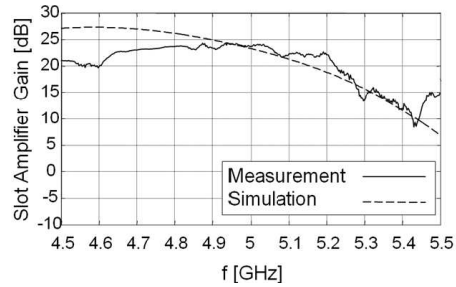


Figure 13. Comparison between simulation and measurement of the QO amplifier gain.

The measurement setup for characterizing the QO slot-amplifier unit cell gain is shown in Fig. 12. The device under test (DUT), containing the isolated unit cell, is illuminated by a WR-187 horn antenna working in the frequency range 3.9 GHz–6 GHz. The horn has a gain of 16.2 dB at 5 GHz. The QO amplifier unit-cell is positioned in the far field region of the horn, at a distance of $R = 1.7$ m. A cross-polarized horn is used as a receiving test antenna, and is identical to the transmitting test radiator, also positioned at a distance of $R = 1.7$ m far from the DUT. Such a configuration allows the determination of the transmission coefficient, S_{21} , from the transmitting horn to the receiving horn, when the slot amplifier is turned on. This measurement requires subsequent elaboration in order to calculate the net contribution of the QO unit cell. If P_T is the power radiated by the transmitting horn and P_R the power actually received by the second horn, then the measured transmission coefficient can be expressed as $S_{21} = P_R/P_T$. In order to extrapolate the real gain of the unit cell, it is important to note that the fraction of the power that is useful for amplification is only a small portion of the total amount radiated by the transmitting horn because the unit-cell area is smaller than the beam aperture at the distance R . To normalize the measurement, let us first consider the half-power beamwidth of the horn, which is equal to $2\varphi = 24^\circ$. The area related to the half-power beamwidth at a distance R is expressed by (1).

$$A_{HP} = L_{HP}^2 = (2R_1 \sin \varphi)^2 \quad (1)$$

being $R_1 = R/\cos \varphi$. As for the unit cell, the area of the manufactured surface is A_{UC} . Hence, the power actually impinging on the amplifier surface is (2):

$$P_{TS} = \frac{P_T}{2} \frac{A_{UC}}{A_{HP}} \quad (2)$$

which means that the real transmission coefficient is (3):

$$S_{21}^S = \frac{P_R}{P_{TS}} = \frac{P_R}{P_T} \left(2 \frac{A_{HP}}{A_{UC}} \right) = S_{21} \left(2 \frac{A_{HP}}{A_{UC}} \right) \quad (3)$$

Once the measured transmission coefficient has been adjusted, the gain of the unit cell can be simply evaluated by inverting the Friis' equation of the system considered from the output interface of the QO amplifier to the receiving horn aperture and it is reported in (4):

$$S_{21}^S = \frac{P_R}{P_{TS}} = G_H^2 G_{TOT} \left(\frac{\lambda}{4\pi R} \right)^2 \quad (4)$$

The unit cell gain is thus (5):

$$G_{TOT_M} = \frac{S_{21}^S}{G_H^2} \left(\frac{4\pi R}{\lambda} \right)^2 \quad (5)$$

where G_H is the gain of the test horn and λ is the free space wavelength.

A comparison between the simulated gain, G_{TOT} , and the measured gain, G_{TOT_M} , of the QO unit cell is reported in Fig. 13. Measured and simulated data are in good agreement within the range 4.75 GHz–5.45 GHz, and show a unit-cell gain of about 24 dB at the operating frequency of 5 GHz. The –3 dB bandwidth estimated from measurements is $BW = 500$ MHz, which correspond to a 10% bandwidth.

5. CONCLUSION

In this work we have proposed a simplified process for designing slot antenna QO amplifier arrays. In the technique proposed, each element of the unit-cell QO amplifier is simulated separately using commercially-available software. The logical division of the design tasks presented here has the aim of simplifying the flow of system synthesis at a preliminary stage. Afterwards, the single elementary blocks can be chained together to model the complete structure. The proposed design approach was validated by fabricating and testing a unit-cell prototype of the QO amplifier in the C-band. The measured results showed a power gain of 24 dB for the single unit cell at 5 GHz and a bandwidth of 10%, both of which values were in good agreement with the simulations.

REFERENCES

1. Mink, J. W., "Quasi-optical power combining of solid state millimeter-wave sources," *IEEE Transactions on Microwave Theory and Techniques*, Vol. 34, 273–279, 1986.

2. Kim, M., et al., "A grid amplifier," *IEEE Microwave and Guided Wave Letters*, [see also *IEEE Microwave and Wireless Components Letters*], Vol. 1, 322–324, 1991.
3. Kim, M., et al., "A 100-element HBT grid amplifier," *IEEE Transactions on Microwave Theory and Techniques*, Vol. 41, 1762–1771, 1993.
4. De Lisio, M., et al., "Modeling and performance of a 100-element pHEMT grid amplifier," *IEEE Transactions on Microwave Theory and Techniques*, Vol. 44, 2136–2144, 1996.
5. Cheung, C.-T., M. P. DeLisio, J. J. Rosenberg, R. Tsai, R. Kagiwada, and D. B. Rutledge, "A single chip two-stage W-band grid amplifier," *IEEE MTT-S International Microwave Symposium Digest*, Vol. 1, 79–82, 2004.
6. Bundy, S. C. and Z. B. Popovic, "A generalized analysis for grid oscillator design," *IEEE Transactions on Microwave Theory and Techniques*, Vol. 42, 2486–2491, 1994.
7. Deckman, B., D. Rutledge, J. J. Rosenberg, E. Sovero, and D. S. Deakin, Jr., "A 1 Watt 38 GHz monolithic grid oscillator," *IEEE MTT-S International Microwave Symposium Digest*, Vol. 3, 1843–1845, 2001.
8. Rahman, M., T. Ivanov, and A. Mortazawi, "A unit cell design for construction of quasi-optical power combining oscillator arrays," *Southcon/96, Conference Record*, 413–415, 1996.
9. Tsai, H. S., M. J. W. Rodwell, and R. A. York, "Planar amplifier array with improved bandwidth using folded slots," *IEEE Microwave and Guided Wave Letters*, Vol. 4, 112–114, 1994.
10. Tsai, H. S. and R. A. York, "FDTD analysis of CPW-fed folded slot and multiple-slot antennas on thin substrates," *IEEE Transactions on Antennas and Propagation*, Vol. 44, 217–226, 1996.
11. Marshall, T., M. Forman, and Z. Popovic, "Two Ka-band quasi-optical amplifier arrays," *IEEE Transactions on Microwave Theory and Techniques*, Vol. 47, 2568–2573, 1999.
12. Tsai, H. S. and R. A. York, "Polarisation-rotating quasi-optical reflection amplifier cell," *Electronics Letters*, Vol. 29, 2125–2127, 1993.
13. Ortiz, S. C., T. Ivanov, and A. Mortazawi, "A CPW-fed microstrip patch quasi-optical amplifier array," *IEEE Transactions on Microwave Theory and Techniques*, Vol. 48, 276–280, 2000.
14. Ortiz, S. C., J. Hubert., L. Mirth, E. Schlecht, and A. Mortazawi, "A high-power Ka-band quasi-optical amplifier array," *IEEE*

- Transactions on Microwave Theory and Techniques*, Vol. 50, 487–494, 2002.
15. Kim, D. and J.-I. Choi, “Analysis of a High-Gain Fabry-PÉrot cavity antenna with an FSS superstrate: Effective medium approach,” *Progress In Electromagnetics Research Letters*, Vol. 7, 59–68, 2009.
 16. Gu, Y. Y., W. X. Zhang, and Z. C. Ge, “Two improved Fabry-Perot resonator printed antennas using EBG substrate and AMC substrate,” *Journal of Electromagnetic Waves and Applications*, Vol. 21, No. 6, 719–728, 2007.
 17. Marcuvitz, N., *Waveguide Handbook*, Peter Peregrinus Ltd., London, UK, 1986.
 18. Nitshisopa, K., J. Nakasuwan, N. Songthanapitak, N. Anantrasirichai, and T. Wakabayashi, “Design CPW fed slot antenna for wideband applications,” *PIERS Online*, Vol. 3, No. 7, 1124–1127, 2007.
 19. Li, Q. and Z. Shen, “Inverted microstrip-fed cavity-backed slot antenna,” *IEEE Antennas and Wireless Prop. Letters*, Vol. 1, 98–101, 2002.
 20. Weller, T. M., L. P. B. Katehi, and G. M. Rebeiz, “Single and double folded-slot antennas on semi-infinite substrate,” *IEEE Transactions on Antennas and Propagation*, Vol. 43, 1423–1428, 1995.
 21. Chen, Y. B., X. F. Liu, Y. C. Jiao, and F. S. Zhang, “A frequency reconfigurable CPW-fed slot antenna,” *Journal of Electromagnetic Waves and Applications*, Vol. 21, No. 12, 1673–1678, 2007.
 22. Ansoft HFSS, Ansoft Corporation.
 23. Virdee, B. S., A. S. Virdee, and B. Y. Banyamin, *Broadband Microwave Amplifiers*, Artech House, London, UK, 2004.
 24. Ansoft Designer/NEXXIM, Ansoft Corporation.